The structure of dark matter halos in hierarchical clustering theories.

Kandaswamy Subramanian

National Centre for Radio Astrophysics, Tata Institute of Fundamental Research, Poona University Campus, Ganeshkhind, Pune 411 007, India.

Renyue Cen and Jeremiah P. Ostriker

Princeton University Observatory, Peyton Hall, Princeton, New Jersey 08544, USA.

ABSTRACT

During hierarchical clustering, smaller masses generally collapse earlier than larger masses and so are denser on the average. The core of a small mass halo could be dense enough to resist disruption and survive undigested, when it is incorporated into a bigger object. We explore the possibility that a nested sequence of undigested cores in the center of the halo, which have survived the hierarchical, inhomogeneous collapse to form larger and larger objects, determines the halo structure in the inner regions. For a flat universe with $P(k) \propto k^n$, scaling arguments then suggest that the core density profile is, $\rho \propto r^{-\alpha}$ with $\alpha = (9 + 3n)/(5 + n)$. For any $n < 1$, the signature of undigested cores is a core density profile shallower than $\rho \propto 1/r^2$ and dependent on the power spectrum. For typical objects formed from a CDM like power spectrum the effective value of n is close to -2 and thus α could typically be near 1, the NFW (see text) value. Also velocity dispersions should deviate from a constant value to decrease with decreasing radius in the core. But whether such behaviour obtains depends on detailed dynamics.

We first examine the dynamics using a fluid approach to the self-similar collapse solutions for the dark matter phase space density, including the effect of velocity dispersions. We highlight the importance of tangential velocity dispersions to obtain density profiles shallower than $1/r^2$ in the core regions. If tangential velocity dispersions in the core are constrained to be less than the radial dispersion, a cuspy core density profile shallower than $1/r$ cannot obtain, in self-similar collapse. We then briefly look at the profiles of the outer halos in low density cosmological models where the total halo mass is convergent. We find a limiting r^{-4} outer profile for the open case and a limiting outer profile for the Λ dominated case, which at late times has the form $[1 - (r/\bar{r}_\lambda)^{-3\epsilon}]^{1/2}$, where 3ϵ is the logarithmic slope of the initial density profile. Finally, we analyze a suite of dark halo density and velocity dispersion profiles obtained in cosmological N-body simulations of models with $n = 0, -1$ and -2. We find that the core-density profiles of dark halos, show considerable scatter in their properties, but nevertheless do appear to reflect a memory of the initial power spectrum, with steeper initial spectra producing flatter core profiles. These results apply as well for

low density cosmological models ($\Omega_{matter} = 0.2 - 0.3$), since high density cores were formed early where $\Omega_{matter} \approx 1$.

Subject headings: Cosmology: dark matter, Large-scale structure of Universe; Galaxies: Formation, Halos, clusters

1. Introduction

In conventional pictures for the growth of structure, galaxies and clusters are thought to originate from the growth of small density fluctuations due to gravitational instability, in a universe dominated by dark matter. In hierarchical clustering models, like the cold dark matter (CDM) models, small mass clumps of dark matter form first and gather into larger and larger masses subsequently. The structure of these dark matter clumps, which we will refer to as "halos", is likely to be related to how the halos formed, the initial spectrum of the density fluctuations and to the underlying cosmology.

Much of the early work on the structure of dark halos concentrated on their density profiles in the outer regions, especially in the context of understanding the flat rotation curves of disk galaxies. The secondary infall paradigm introduced by Gunn and Gott (1972) and subsequently amplified by Fillmore and Goldreich (FG, 1984) and Bertschinger (B85, 1985) suggests that gravitational collapse around a seed perturbation will generically lead to divergent extended halos which produce a nearly flat rotation curve in the outer regions for the case $\Omega_{matter} \equiv \Omega_m = 1$. The Gunn-Gott picture would lead to steep convergent profiles in the outer regions for low density ($\Omega_m < 1$) universes. If current estimates for the global density parameter are correct ($\Omega_m = 0.3 \pm 0.1$), then the high density core ($\rho_{core}/ < \rho >> 10^3$) were formed early enough so that the $\Omega_m = 1$ picture effectively applies. But the outer halos represent the current, low density universe.

The nature of the density profiles of dark halos in the inner regions is also of importance from several points of view. The structure of dark halo cores determines the efficiency of gravitational lensing by the galactic and cluster halos, the X- ray emissivity of clusters and galactic rotation curves in the inner regions. These properties of galactic and cluster halos can be well constrained by observations. So, if the core density profile of dark halos are fossils which do depend on some of the properties of structure formation models, like their initial power spectrum, one would have a useful observational handle on these properties. It is therefore necessary to understand what determines the nature of the density profiles of dark matter halos, and their cores, *ab initio*. We discuss this issue here.

Further, Navarro, Frenk and White (NFW) (1995, 96, 97) have proposed from their N-body simulations, that dark matter halos in hierarchical clustering scenarios develop a universal density profile, regardless of the scenario for structure formation or cosmology. The NFW profile has an

inner cuspy form with the density $\rho \propto r^{-1}$ and an outer envelope of the form $\rho \propto r^{-3}$. There does not appear to be any reason, apriori, why halo density profiles should prefer such a form, but empirically, several investigators have found that the NFW profile provides a moderately good fit to numerical simulations (Cole and Lacey 1996, Tormen, Bouchet & White 1997, Huss, Jain & Steinmetz 1997, 1999, Thomas *et al.*, 1998). Recently, though, high resolution simulations of cluster formation in a CDM model, by Moore *et al.* (1998), yielded a core density profile $\rho(r) \propto r^{-1.4}$, shallower than r^{-2}, but steeper than the r^{-1} form preferred by NFW, consistent with the earlier high resolution work of Xu (1995). A similar result was also found earlier by Fukushige and Makino (1997). (For small mass halo cores on the other hand, Kravtsov *et al.* (1998), find an average core density profile, shallower than the NFW form). Xu (1995) also found that there was a large scatter in the the logarithmic slope of halo density profiles in both the core and outer regions. One motivation of our work was to examine this issue on general theoretical grounds; while at the same time check in some of our own numerical experiments, the properties of dark halo density and velocity dispersion profiles.

In the next section we discuss the processes which may determine the halo density profile and consider the role of undigested cores in setting the structure of dark halos cores. For a flat universe with $P(k) \propto k^n$, scaling arguments suggest that $\rho \propto r^{-\alpha}$ with $\alpha = \alpha_n = (9 + 3n)/(5 + n)$. As an aside we note here that for popular cosmological models $n \approx -2$, in the appropriate range of wavelengths, giving $\alpha = 1$, the NFW value. But whether such a scaling law indeed obtains depends on the detailed dynamics.

In order to explore the dynamical issues, we consider first self similar collapse of a single spherically symmetric density perturbation, in a scale free universe. We introduce a fluid approach for analyzing this problem, in Section 3. We highlight the importance of tangential velocity dispersions to obtain density laws shallower than $1/r^2$ in the core regions. In a companion paper (Subramanian, 1999, S99 henceforth), one of us (KS) considers these self-similar collapse solutions in greater detail, by deriving and solving numerically the scaled moment equations for such a collapse, including the effect of tangential velocity dispersions.

In Section 4 we analyze, following the Gunn-Gott paradigm, the outer profiles expected in low density universes, where an outer profile steeper than r^{-3} must obtain. In Section 5, we analyze dark halo density and velocity dispersion profiles obtained in cosmological N-body simulations of models with $n = 0, -1$ and -2. We show that the core-density profiles of dark halos, show some scatter in their properties, but nevertheless do appear to reflect a memory of the initial power spectrum. The final Section discusses the results and presents our conclusions.

2.   The density profiles of dark halos

To fix ideas, let us limit ourself initially, to the Einstein de-Sitter universe, with $\Omega = 1$. This is almost certainly not the correct cosmological model, but it provides a convenient context within

which to discuss the formation of structure and it is likely to be a very good approximation at epochs $(1 + z) > \Omega_m^{-1}$ at which the cores of familiar objects have formed. Let us also assume that the Fourier space power spectrum of density fluctuations is a power law, $P(k) = Ak^n$, where the spectral index n lies between the limits $-3 < n < 1$. In this case structure grows hierarchically with small scales going non-linear first and larger and larger mass scales going non-linear at progressively later times. For such a scale free universe, all properties of dark matter distributions at each epoch are just a scaled version of those in previous epochs i.e. the universe is self-similar. What would decide the density profile of a dark matter halo in such a cosmological setting?

It is likely that at least three processes are important. Firstly, when some mass scale decouples from the general Hubble expansion and collapses in an inhomogeneous fashion to form a dark matter halo, the changing gravitational potential and phase mixing will cause some amount of violent relaxation or " virialisation" to occur. A general constraint on the equilibrium distribution of such a halo will be set by energy and mass conservation together with scaling laws which obtain in a hierarchical clustering scenario.

Secondly, in the cosmological context, a collapsed mass is not isolated and will therefore continue to accrete surrounding material, as long as matter dominates the energy density. Such a secondary infall onto the collapsed halo will alter/determine its structure in the outer regions.

We emphasize here a third process: When any mass scale collapses, in a hierarchical theory, it will already contain a dominant smaller mass dark halo which collapsed earlier, and is therefore denser on the average. Typically the core of such a smaller mass halo, is dense enough to resist disruption and survive undigested, when it is incorporated into the bigger object. A nested sequence of undigested cores in the center of the halo, which have survived the hierarchical inhomogeneous collapse to form larger and larger objects, could thus determine the halo structure in the inner regions. We illustrate this idea schematically in Figure 1.

Suppose a halo of mass M collapses to form a "virialised" object with a characteristic density ρ_0 and core radius r_c. For $P(k) \propto k^n$, simple standard scaling arguments using linear theory (cf. Peebles 1980, Padmanabhan and Subramanian 1992, Padmanabhan 1993), predict that ρ_0 and r_c, scale with mass M as

$$\rho_0(M) \propto M^{-(n+3)/2}; \qquad r_c(M) \propto M^{(n+5)/6}; \qquad \rho_0 \propto r_c^{-(9+3n)/(5+n)} \tag{1}$$

So, in the above sequential collapse to form larger and larger objects, the undigested core of each member of the sequence, typically contributes a density ρ_0 at a scale r_c, satisfying the the relation $\rho_0 = c_1 r_c^{-(9+3n)/(5+n)}$, with some constant c_1.

This suggests that the inner density profile of the bigger halo, which is the envelope of the profiles of the nested sequence of smaller mass cores could have the form

$$\rho(r) \propto r^{-\alpha}, \qquad \alpha = \alpha_n = \frac{9 + 3n}{5 + n} \tag{2}$$

Note that for any $n < 1$, $\alpha < 2$. So one expects the core density profile to have a power law

dependence, shallower than r^{-2}, when smaller mass cores remain undigested in the formation of a larger mass. It is intriguing that the same form for the *density profile* (as against the correlation function) is also argued for by Peebles (1980; section 26.). In a paper which appeared during the course of this work Syer & White (1998) give a similar argument, for the case when bigger halos form by purely mergers of smaller halos. Our argument (concluding with equation (2)) of course neglects both previous generation of undigested cores and secondary infall and is only designed to model the innermost part of a currently virializing object, where their effects on the energetics should be minimal.

One can also state the above argument in terms of the velocity dispersion or the rotation velocity profiles. The typical velocity dispersion of a collapsed halo $\sigma \propto (M/r_c)^{1/2}$. Since the scaling argument gives $r_c \propto M^{(n+5)/6}$, we therefore have $\sigma^2 \propto r_c^{(1-n)/(5+n)}$. So for any $n < 1$, smaller mass objects have a smaller velocity dispersion and higher phase space densities than larger mass objects. The survival of a nested sequence of cores during the inhomogeneous collapse to form bigger and bigger objects, then suggests that the velocity dispersion profile in the core regions will scale as $\sigma^2(r) \propto r^{(1-n)/(5+n)}$. For any $n < 1$, an alternate signature of undigested cores is then a velocity dispersion which decreases with decreasing radius in the above fashion. It is interesting to note in this context that, the cluster scale halo core in the Moore *et al.* (1998) simulation, does indeed show such a velocity dispersion profile, with σ decreasing with decreasing r (Moore, private communication).

We have assumed above that each stage of the hierarchy arises from a typical density fluctuation. In general there would be a scatter in the sub-halo properties since the initial density peaks heights are random with a Gaussian probability distribution. This will lead to a scatter in the slope α, for any individual halo (cf. Nusser and Sheth 1999 and section 5 below).

The arguments so far have been semi-quantitative but general. We consider, in the next section, another approach to the density profiles of halo cores via spherically symmetric, self similar collapse solutions to the Vlasov equation. Our motivation is to see whether the results derived above, can be recovered in any simple, analytically tractable model. This model will also allow us to examine, in a simple setting, the dynamical constraints on obtaining core density profiles of the form given by Eq. (2).

3.   Self similar collapse and halo density profiles: a fluid approach

Consider the collapse of a single spherically symmetric density perturbation, in a flat background universe. Suppose the initial density fluctuation is a power law in radius. Then there is no special scale in the problem either from initial conditions or cosmology. We expect to be able to describe the further evolution of such a density perturbation, through a self similar solution. FG and B85 looked at purely radial self similar collapse by solving for the self similar particle trajectory. We adopt a different approach here, examining directly the evolution of the

distribution function of the dark matter. During the course of this work we learned that a number of authors (Padmanabhan 1994, unpublished notes; Padmanabhan 1996a, Chieze, Teyssier & Alimi 1997, Henriksen & Widrow 1997) have also adopted this approach to the self similar collapse problem considered by FG and B85. We will emphasize here also the role of non-radial motions in self similar collapse solutions.

3.1. The self similar solution

The evolution of dark matter phase space density $f(\mathbf{r}, \mathbf{v}, t)$ is governed by the Vlasov Equation,

$$\frac{\partial f}{\partial t} + \mathbf{v}.\frac{\partial f}{\partial \mathbf{r}} + \mathbf{a}.\frac{\partial f}{\partial \mathbf{v}} = 0, \tag{3}$$

where $\mathbf{r}$ and $\mathbf{v} = \dot{\mathbf{r}}$ are the proper co-ordinate and velocity of the particles respectively. Also the acceleration $\mathbf{a} = \dot{\mathbf{v}} = -\nabla\Phi$, with

$$\nabla^2\Phi = 4\pi G\rho = 4\pi G \int f d^3\mathbf{v}. \tag{4}$$

By direct substitution, it is easy to verify that these equations admit self similar solutions of the form

$$f(\mathbf{r}, \mathbf{v}, t) = k_2 k_1^{-3} t^{-q-2p} F(\frac{\mathbf{r}}{k_1 t^p}, \frac{\mathbf{v}}{k_1 t^q}); \qquad p = q + 1, \tag{5}$$

where k_1, k_2 are constants which we will fix to convenient values below.

We have used proper co-ordinates here since the final equilibrium halo is most simply described in these co-ordinates. (The same solution in co-moving co-ordinates for the density is given by Padmanabhan (1996a)). Defining a new set of co-ordinates $\mathbf{y} = \mathbf{r}/(k_1 t^p)$, $\mathbf{w} = \mathbf{v}/(k_1 t^q)$ and a scaled potential $\chi = k_1^{-2} t^{-2q}\Phi$, the scaled phase space density F satisfies

$$- (q + 2p)F - p\mathbf{y}.\frac{\partial F}{\partial \mathbf{y}} - q\mathbf{w}.\frac{\partial F}{\partial \mathbf{w}} + \mathbf{w}.\frac{\partial F}{\partial \mathbf{y}} - \nabla_{\mathbf{y}}\chi.\frac{\partial F}{\partial \mathbf{w}} = 0; \tag{6}$$

$$\nabla_{\mathbf{y}}^2\chi = 4\pi G k_2 \int F d^3\mathbf{w}. \tag{7}$$

Consider the evolution of a spherically symmetric density perturbation, in a flat universe whose scale factor $a(t) \propto t^{2/3}$. For self similar evolution, the density is given by

$$\rho(r, t) = \int f d^3\mathbf{v} = k_2 t^{2q-2p} \int F(y, \mathbf{w}) d^3\mathbf{w} = k_2 t^{-2} \int F(y, \mathbf{w}) d^3\mathbf{w} \equiv k_2 t^{-2}\psi(y) \tag{8}$$

where we have defined $r = |\mathbf{r}|$, $y = |\mathbf{y}|$ and used the relation $p = q + 1$. For the flat universe, the background matter density evolves as $\rho_b(t) = 1/(6\pi G t^2)$. So the density contrast $\rho(r, t)/\rho_b(t) = \psi(y)$, where we take $k_2 = 1/(6\pi G)$.

3.2. Linear and non-linear limits

Let the initial excess density contrast averaged over a sphere of co-moving radius $x = r/a(t) \propto rt^{-2/3}$ be a power law $\bar{\delta}(x, t_i) \propto x^{-3\epsilon}$. Since ρ/ρ_b is a function of y alone, the $\bar{\delta}(x, t)$ will also be a function only of y. Note that, in the linear regime, it is the excess density contrast averaged over a *co-moving* sphere, which grows as the scale factor $a(t)$. So one can write for the linear evolution of the spherical perturbation

$$\bar{\delta}(r, t) = \bar{\delta}_0 x^{-3\epsilon} t^{2/3} = \bar{\delta}_0 r^{-3\epsilon} t^{2/3 + 2\epsilon} = \bar{\delta}_0 y^{-3\epsilon} t^{-3\epsilon p + 2/3 + 2\epsilon}, \tag{9}$$

where we have substituted $r = yt^p$. This can be a function of y alone, for a range of t in the linear regime iff $-3\epsilon p + 2/3 + 2\epsilon = 0$, which gives

$$p = \frac{2 + 6\epsilon}{9\epsilon}. \tag{10}$$

We see that once the initial density profile is specified, the exponents p, q of the self similar solution are completely determined. (For an initial $\bar{\delta}(x, t_i) \propto x^{-3\epsilon}$, the radius of the shell turning around at time t is, $r_t(t) \propto t^p$. So a natural way of fixing the constant k_1 is by taking $k_1 t^p = r_t(t)$, and $y = r/r_t(t)$. We will do this in what follows.)

Consider now what happens in the non-linear limit. The zeroth moment of the Vlasov equation gives

$$\frac{\partial \rho}{\partial t} + \nabla_{\mathbf{r}}.(\rho \bar{\mathbf{v}}) = 0 \tag{11}$$

Here $\bar{\mathbf{v}}$ is the mean velocity (first moment of f over the velocity). In the non-linear regime, one expects, each shell of dark matter, which was initially expanding, to turn around, after reaching a maximum radius and collapse. Subsequently the shell would oscillate between a minimum radius, which depends on how much non-radial velocities the shell particles have and a maximum radius, which depends on how the mass within the shell grows with time. In regions which have had a large amount of shell crossings, the halo particles have settled to nearly zero average infall velocity, that is $\bar{v}_r = 0$. (They could of course still have velocity dispersions). Using $\bar{v}_r \equiv 0$ in (11), we have $(\partial \rho / \partial t) = 0$, in the non-linear regime. In this regime therefore,

$$\rho(r, t) = Q(r) = Q(yt^p) = \frac{1}{6\pi G t^2} \psi(y) \tag{12}$$

This functional equation has only power law solution, because of the power law dependences on t. Substituting $Q(r) = q_0 r^{-\alpha}$ into Eq. (12), and using $r \propto yt^p$, we obtain $y^{-\alpha} t^{-p\alpha} \propto t^{-2} D(y)$. This can only be satisfied for range of t in the non-linear regime provided $p\alpha = 2$. So, for an initial density profile with a power law slope 3ϵ, the power law slope of the density in the non-linear regime is given by,

$$\alpha = \frac{2}{p} = \frac{9\epsilon}{3\epsilon + 1}. \tag{13}$$

B85 considered the self-similar secondary infall onto an initially localised, overdense perturbation, corresponding to taking $\epsilon = 1$. Using Eq. (13) this gives $\alpha = 9/4$, the slope for

the density at the non-linear end deduced by following the self similar particle trajectory. FG considered a range of ϵ and our value of α agrees with that obtained by them, again by following particle trajectories. Both these authors also restricted themselves to purely radial orbits. In this case FG argued that while the above form for α should obtain for $2/3 \le \epsilon < 1$, for $\epsilon < 2/3$, one goes to the limiting value $\alpha = 2$. However, this is only true for purely radial trajectories (cf. White and Zaritsky 1992; Sikvie, Tkachev & Wang 1997). We will also see below, by considering the higher moments of the Vlasov equation, that $\alpha < 2$ can only obtain if the system has non-radial velocity dispersions.

What should we choose for the value of ϵ? For a power law $P(k) \propto k^n$, the fractional density contrast averaged over a co-moving sphere of radius x, is distributed as a Gaussian, with a variance $\propto x^{-(3+n)/2}$ (cf. Peebles 1980). This suggests a "typical" spherically averaged initial density law for a halo collapsing around a randomly placed point of the form $\bar{\delta}(x, t_i) \propto x^{-(3+n)/2}$, or $3\epsilon = (3+n)/2$. Suppose we use this value of ϵ for the initial density profile of a halo. Then in the non-linear stage, the halo density in regions which have settled down to a zero mean radial velocity, will be $\rho(r,t) \propto r^{-\alpha}$, where, using $3\epsilon = (3+n)/2$ in Eq. (13)

$$\alpha = \alpha_n = \frac{9 + 3n}{5 + n} \tag{14}$$

This result should obtain for collapses from power law initial power spectrum. Remarkably, this is the same law we derived earlier for the core of a collapsed halo, assuming that the cores of sequence of sub-halos are left undigested, during the formation of the bigger halo.

An alternate choice, $3\epsilon = (3+n)$ would be relevant if one were considering the collapse around an isolated high density peak; since in this case the initial density profile would be proportional to the correlation function to lowest order (cf. Bardeen *et al.* 1986). In this case one gets $\alpha = (9+3n)/(4+n)$ (Hofmann & Shaham 1985, Padmanabhan 1996b). (Since $\epsilon < 1$ for overdense perturbations, we can use this choise only for $n < 0$).

Note that for $n < 1$ the density law given by (14) is shallower than $1/r^2$, which was claimed to be a limiting form by FG in case of radial collapse. To see how such a restriction comes about and when one can obtain a shallower slope than r^{-2} for the halo cores, it is interesting to consider the higher moments of the Vlasov equation (the Jeans equations) for the spherical self similar solution.

3.3. A fluid approach to collisionless dynamics

Suppose we multiply the Vlasov equation by the components of $\mathbf{v}$ and integrate over all $\mathbf{v}$. In regions where large amounts of shell crossing have occurred, one can assume that a quasi "equilibrium" state obtains, whereby all odd moments of the distribution function, over $(\mathbf{v} - \bar{\mathbf{v}})$, may be neglected. Assume there is no mean rotation to the halo, that is $\bar{v}_\theta = 0$ and $\bar{v}_\phi = 0$. Then

we get

$$\frac{\partial(\rho \bar{v}_r)}{\partial t} + \frac{\partial(\rho \bar{v_r^2})}{\partial r} + \frac{\rho}{r}(2\bar{v_r^2} - \bar{v_\theta^2} - \bar{v_\phi^2}) + \frac{GM(r)\rho}{r^2} = 0; \tag{15}$$

$$\bar{v_\theta^2} = \bar{v_\phi^2}. \tag{16}$$

Here $M(r)$ is the mass contained in a sphere of radius r.

For a purely radial collapse we can set $\bar{v_\theta^2} = \bar{v_\phi^2} = 0$. Let us also assume to begin with that one can set $\bar{v}_r = 0$, in the inner parts. Then integrating the Jeans equation (15), with $\rho = q_0 r^{-\alpha}$ gives

$$\bar{v_r^2} = r^{2-\alpha}\left[\frac{4\pi G q_0}{2(\alpha-2)(3-\alpha)}\right] \equiv \frac{1}{(\alpha-2)}\frac{GM(r)}{2r}. \tag{17}$$

So purely radial self-similar collapse with no tangential velocities, and with $\alpha > 2$, leads to a radial velocity dispersion in the core which scales as $\bar{v_r^2} \propto r^{-(\alpha-2)}$. This agrees with the radial velocity dispersion scaling as $r^{-1/8}$ for B85 gaseous collapse solution. ($\alpha = 2$ needs to be treated separately). Further the RHS of Eq. (17) should be necessarily non-negative, which is violated when $\alpha < 2$. If one has a purely spherically symmetric collapse and zero tangential velocities, then the density law cannot become shallower than $\alpha = 2$ and maintain a static core with $\bar{v}_r = 0$. This agrees with FG. Our example illustrates a point we mentioned earlier. Even if simple scaling arguments suggest a $\alpha < 2$ possibility, there could be dynamical restrictions for realizing such core profiles.

Let us now include the effect of tangential velocity dispersions. The Jeans equation gives two equations for the three unknown velocity dispersions, even for a static core. To see if one can close the system let us look at the second moments of the Vlasov equation (the energy equations) We get

$$\frac{\partial(\rho \bar{v_\theta^2})}{\partial t} + \frac{1}{r^4}\frac{\partial(\rho r^4 <v_r v_\theta^2>)}{\partial r} - \frac{2\rho <v_\theta v_\phi^2> \cot\theta}{r} + \frac{\rho \bar{v_\theta^3}\cot\theta}{r} = 0, \tag{18}$$

$$\frac{\partial(\rho \bar{v_\phi^2})}{\partial t} + \frac{1}{r^4}\frac{\partial(\rho r^4 <v_r v_\phi^2>)}{\partial r} + \frac{\rho <v_\theta v_\phi^2> \cot\theta}{r} = 0, \tag{19}$$

$$\frac{\partial(\rho \bar{v_r^2})}{\partial t} + \frac{1}{r^2}\frac{\partial(\rho r^2 \bar{v_r^3})}{\partial r} - \frac{2\rho <v_r(v_\theta^2 + v_\phi^2)>}{r} + 2\bar{v}_r \rho GM/r^2 = 0, \tag{20}$$

where $M = \int 4\pi r^2 \rho$ is the mass within r and both $<>$ or a bar over a variable denotes a normalized moment over f.

Consistent with our statistical assumption for the core regions, we assume that initially the tangential velocities have zero skewness. Then in purely spherically symmetric evolution they would not develop any skewness, that is $\bar{v_\theta^3} = \bar{v_\phi^3} = <v_\theta v_\phi^2> = 0$ for all times. Also if the initial velocity ellipsoid had one of its principle axis pointing radially, we do not expect this axis to become misaligned in purely spherical evolution. This means we can assume $<v_r v_\theta^2> = \bar{v}_r \bar{v_\theta^2} = 0$ in the static core. Eq. (18) then implies $(\partial(\rho \bar{v_\theta^2})/\partial t) = 0$ or $\rho \bar{v_\theta^2} = K(r)$ independent of t. For

the scaling solution we then have

$$\rho \bar{v}_\theta^2 = K(r) = K(yt^p) = k_2 k_1^2 t^{4q-2p} \int w_\theta^2 F(y, \mathbf{w}) d^3\mathbf{w}. \tag{21}$$

Once again substituting a power law solution $K(r) = K_0 r^s$, to this functional equation, we get the constraint from matching power of t on both sides, $ps = 4q - 2p$. Using $p = q + 1$, we then get $s = 2 - 4/p = 2 - 2\alpha$, and so

$$\rho \bar{v}_\theta^2 = K_0 r^{2-2\alpha}. \tag{22}$$

Integrating the radial momentum equation using Eq. (15), (16), (22) and using $\rho = q_0 r^{-\alpha}$. Equation (17) for the radial velocity dispersion is now altered to

$$\bar{v}_r^2 = r^{2-\alpha} \left[\frac{K_0}{(2-\alpha)q_0} - \frac{4\pi G q_0}{2(2-\alpha)(3-\alpha)} \right] \equiv \frac{1}{(2-\alpha)} \left[\bar{v}_\theta^2(r) - \frac{GM(r)}{2r} \right]. \tag{23}$$

Several important points are to be noted from the above equation. A crucial one is that, when $\alpha < 2$, the RHS of Eq. (23) can remain positive, only provided that one has a non zero tangential velocity dispersion. In fact, for any $\alpha < 2$, one needs the tangential velocity dispersion to be at least as large as $GM/2r$, comparable to the gravitational potential energy per unit mass. Also one can see that to obtain static cores with $\alpha < 1$, the required tangential dispersion must be larger than the radial velocity dispersion. So if in halo cores tangential velocity dispersions are constrained to be smaller than radial velocity dispersions, then a core density profile shallower than $1/r$ cannot obtain in the self-similar case. Also note that for $\alpha < 2$, all the components of velocity dispersions decrease with decreasing radius, as suggested by the simple scaling arguments of the previous section.

In a realistic collapsing halo it is quite likely that particles develop non-radial velocities. Tidal forces by mass concentrations outside the halo and the presence of substructure within the collapsing halo will lead to non-radial motion of particles. More generally the process of violent relaxation during the inhomogeneous collapse to form the halo will lead to a more isotropic velocity dispersion.

The above results for the halo core arise simply from the properties of the self similar solution and the assumption of a static core. From the energy equation (20) we note that a time independent radial velocity dispersion, can only obtain if the radial velocity skewness $< (v_r - \bar{v}_r)^3 >$ is also zero. Note that in the core regions where large amounts of shell crossing has occurred, as we stated earlier, the radial skewness is indeed expected to be small. So for the core regions one can in fact make this statistical assumption. Such a treatment will correspond to considering a fluid like limit to the Vlasov equation.

However, the radial skewness will become important near the radius, where infalling matter meets the outermost re-expanding shell of matter. This region will appear like a shock front in the fluid limit. A possible treatment of the full problem in the fluid approach to the Vlasov equation

then suggests itself. This is to take the radial skewness to be zero both inside and outside a "shock or caustic" radius, whose location is to be determined as an eigenvalue, so as to match the inner core solution that we determine in this section with an outer spherical infall solution. One has to also match various quantities across this "shock", using jump conditions, derived from the equations themselves. To do this requires numerical solution of the self consistent set of moment equations, to the scaled Vlasov equation. The details of such a treatment are given a companion paper (Subramanian 1999, S99). Here we summarise the general conclusions of this work.

The numerical results in S99 shows the importance of tangential velocity dispersions, in deciding whether the self similar solution, with an initial density profile shallower than $1/r^2$ ($\epsilon < 2/3$) retains a memory of this initial profile or whether the density profile tends to a universal $1/r^2$ form. The set of solutions show that for a large enough $\bar{v}_\theta^2/\bar{v}_r^2 > 1$, the the core density profile is indeed close to the form $\rho \propto r^{-\alpha}$, with $\alpha = 9\epsilon/(1 + 3\epsilon)$. For $\bar{v}_\theta^2/\bar{v}_r^2 \sim 1$, some memory of the initial density profile is always retained; the density profile has an asymptotic form $\rho \propto r^{-\bar{\alpha}}$, with $\alpha < \bar{\alpha} < 2$. When $\bar{v}_\theta^2/\bar{v}_r^2 << 1$, the density profile goes over to the $1/r^2$ form derived by FG. Also for very shallow initial density profiles with $\alpha < 1$, one must necessarily have a tangential dispersion much larger than radial dispersion to get a static core region, retaining the memory of the initial density profile.

The spherical self similar collapse solutions provide a useful means of examining the dynamics of dark halo formation, and its implications for the core-density profiles, although limited by the spherical symmetry assumption. A complimentary approach would be direct cosmological N-Body simulations of halo formation, which we will consider in Section 5. Before this, we consider briefly below, the outer profiles of dark halos, especially in low density universes.

4. Outer profiles of dark halos

In the cosmological context, as mentioned in section 2, any collapsed mass will continue to accrete surrounding material, as long as the matter density dominates the energy density. We now analyze the consequence of such secondary infall for the outer profile of halos, following the Gunn-Gott paradigm, relaxing the restriction of a flat universe.

Consider the collapse a spherically symmetric density perturbation, in a universe with present matter density parameter Ω_m and cosmological constant Λ. Let the initial density distribution (at time t_i), be $\rho(r, t_i) = \rho_b(t_i)(1 + \delta_i(r))$, and initial velocity of the perturbation be the Hubble velocity. Here $\rho_b(t)$ is the matter density of the smooth universe, and δ_i the initial fractional density contrast of the perturbation, as before. Consider a spherical shell initially at a radius r_i. The evolution of the proper radius $r(t)$ of any such shell before shell crossing is governed by

$$\frac{1}{2}\left(\frac{dr}{dt}\right)^2 - \frac{GM}{r} - \frac{\Lambda r^2}{6} = E(M). \tag{24}$$

Here $M = \rho_b(t_i)(4\pi r_i^3/3)(1 + \bar{\delta}_i)$, is the mass enclosed by the shell and

$$\bar{\delta}_i(r_i) = \frac{3}{r_i^3} \int_0^{r_i} \delta_i(u)u^2 du \tag{25}$$

is the spherically averaged value of $\delta_i(r)$ within r_i. The "energy" $E(M)$ can be fixed by evaluating the LHS of Eq. (24) at the initial time. The shell will turn around at a time say t_m, when $dr/dt = 0$, and its radius is say $r(t_m, r_i) \equiv R(r_i)$. Setting $dr/dt = 0$ in Eq. (24) gives

$$\frac{(1 + \bar{\delta}_i)}{y} + y^2\lambda = \lambda - (\Omega_{mi}^{-1} - 1) + \bar{\delta}_i = \bar{\delta}_i + \frac{(\Omega_t - 1)}{\Omega_{mi}}, \tag{26}$$

where the total value of Ω (including the cosmological constant) is $\Omega_t = \Omega_{mi}(1 + \lambda)$. Here $y \equiv R(r_i)/r_i$ and $\lambda = \Lambda/(3H_i^2\Omega_{mi})$ with H_i the Hubble parameter and Ω_{mi} the matter density parameter at the initial time t_i.

Let us begin with the case $\Lambda = 0$. Then Eq. (26) gives

$$y \equiv \frac{R(r_i)}{r_i} = \frac{(1 + \bar{\delta}_i)}{\bar{\delta}_i - \delta_c}, \tag{27}$$

where we define $\delta_c \equiv (\Omega_{mi}^{-1} - 1)$. In an open universe with $\Omega_{mi} < 1$, one needs $\bar{\delta}_i > \delta_c$ for a shell to turn around and collapse. For a monotonically decreasing initial density profile, there will then be an outer most shell with an initial radius r_c, satisfying $\bar{\delta}_i(r_c) = \delta_c$, such that only shells with $r_i < r_c$, can recollapse onto the density perturbation. To work out the outer profile after collapse, we need to know the final effective radius $r(R)$, of a shell turning around at radius R. Following the Gunn-Gott picture, we assume that these two radii can be related by $r(R) = f_0 R$, where f_0 is some constant. Note that f_0 is indeed a constant if the collapse is exactly self similar, and the initial density profile is sufficiently steep (Section 3, with $\epsilon > 2/3$). For deriving the dominant scaling of the outer profile with radius, even in an open universe, it should also suffice to treat it to be approximately constant (see below). Consider an initial density profile with $\bar{\delta}_i(r_i) = d_0(r_i/r_0)^{-3\epsilon}$. Then using mass conservation, $4\pi r^2 dr \rho(r) = 4\pi r_i^2 dr_i \rho_b(t_i)(1 + \delta_i)$, and the final density profile $\rho(r)$ after collapse is given by

$$\rho(r) = \frac{\rho_b(t_i)}{f_0^3} \frac{\bar{\delta}_i^3(r_i) \left[1 - (r_i/r_c)^{3\epsilon}\right]^4}{\left[1 + 3\epsilon - (r_i/r_c)^{3\epsilon}\right]} \tag{28}$$

with

$$r_i = r\frac{\bar{\delta}_i[1 - (r_i/r_c)^{3\epsilon}]}{f_0} \tag{29}$$

(Here we have also assumed that the initial $\delta_i << 1$.)

Two limits are of interest. First, for a flat matter dominated universe we have $\delta_c = 0$ and $r_c \to \infty$. Then $[1 - (r_i/r_c)^{3\epsilon}] \to 1$ and we recover the standard result

$$\rho(r) = \frac{\rho_b(t_i)}{1 + 3\epsilon} \left(\frac{d_0}{f_0}\right)^{3/(1+3\epsilon)} \left(\frac{r}{r_0}\right)^{-9\epsilon/(1+3\epsilon)}. \tag{30}$$

For $\epsilon = 1$, which is the steepest possible value obtaining for an initially localised overdense perturbation, we recover a halo profile $\rho(r) \propto r^{-9/4}$ (B85 and Section 3).

Now we return to the case of an open universe but examine the outermost profile where $r_i \to r_c$, the critical radius. In this case, from (28) and (29), the outer profile at large radii is given by

$$\rho(r) \to \frac{\rho_b(t_i)f_0}{3\epsilon\delta_c} \left(\frac{r}{r_c}\right)^{-4}, \tag{31}$$

the slope being independent of the initial power law slope ϵ. This interesting result seems to have been already known to Gunn (1977), but not much emphasised since then. As the outer profile in this case is also a pure power law, it is likely that our assumption of a constant f_0 is valid in this case. It would be of interest to find an exact similarity solution of the form given in Section 3, and valid in an open universe which recovers this outer profile.

Let us now turn to the currently popular flat cosmological models with $\Lambda \neq 0$. First from Einstein's equation for the scale factor, we have $\lambda - \Omega_{mi}^{-1} + 1 = 0$ (or $\Omega_t = 1$). Using this and taking $\bar{\delta}_i << 1$, Eq. (26) for $R(r_i)$ becomes

$$\frac{1}{y} + y^2\lambda = \bar{\delta}_i. \tag{32}$$

For a monotonically decreasing $\bar{\delta}_i(r_i)$, the RHS of (32) monotonically decreases. However the LHS as a function of y has a minimum value at $y = y_c = (2\lambda)^{-1/3}$, which is given by $\delta_\lambda = (3/2)(2\lambda)^{1/3}$. There again exists a critical radius r_λ defined by $\bar{\delta}_i(r_\lambda) = \delta_\lambda$, such that, only those shells with $r_i < r_\lambda$ will be able to turn around and collapse. For shells with initial radii $r_i > r_\lambda$, the repulsion due to the cosmological constant overcomes the attractive gravitational force, and so they expand for ever. (The critical value of $y = y_c$ can also be written as $y_c = 3/(2\delta_\lambda)$, a limit got by Barrow and Saich (1993; eq. 26)). Although this feature is similar to the open universe case, there is a major difference between the open model and the flat universe with a cosmological constant. In the Λ dominated model, even for the limiting case $r_i \to r_\lambda$ the turn around radius tends to a finite limit, $R(r_i) \to r_\lambda y_c$. In the open model on the other hand, as $r_i \to r_c$, (the limiting critical radius beyond which shells expand for ever), $\bar{\delta}_i \to \delta_c$, and $R(r_i) \propto (\bar{\delta}_i - \delta_c)^{-1} \to \infty$. But in both cases the accreted mass is finite and equal to that initially within r_c or r_λ.

Let us now consider the limiting denity profile about this outer most cut off radius, for the Λ dominated model. For this, it is sufficient to consider values of r_i close to but less than r_λ and expand the LHS of Eq. (32), about $y = y_c$, retaining upto quadratic terms in $(y - y_c)$. We then have for the outermost shells $\delta_\lambda + 3\lambda(y - y_c)^2 = \bar{\delta}_i(r_i)$ or

$$R(r_i; r_i \to r_\lambda) = r_i y_c - (3\lambda)^{-1/2} \left[\bar{\delta}_i(r_i) - \delta_\lambda\right]^{1/2} r_i, \tag{33}$$

where the negative square root has to be taken as the turn around radii for the collapsing shells are smaller than the maximum value of $R = r_\lambda y_c$. For computing the collapsed density profile, we need again the relation between the turn around radius and the final effective radius. For

a Λ dominated model, it is known that f_0, the ratio of the effective "virial" radius to the turn around radius, depends on the turn around radius itself, that is $r = f_0(R)R$ (Lahav et $al.$ 1991; Barrow and Saich 1993). So $dr/dr_i = f_0(dR/dr_i)(1 + c_1)$, where $c_1 = d(ln(f_0))/d(ln(R))$. Let us assume the power law form of $\bar{\delta}_i(r_i)$ given above. From mass conservation once again $\rho(r) = \rho_b(t_i)(r_i/R)^2(dr_i/dR)f_0^{-3}(1 + c_1)^{-1}$. From Eq. (33), in the limit of $r_i \to r_\lambda$, which is the limit relevant for evaluating the outer profile, $(r_i/R) \to y_c^{-1}$ a finite value. However from this equation $dr_i/dR \to 0$ and the outer density profile cuts off as one nears a critical radius. Using Eq. (33) the limiting outer halo density profile becomes

$$\rho(r) \to \frac{4\lambda\rho_b(t_i)}{3\epsilon f_0^3(1 + c_1)}\left[1 - (r/\bar{r}_\lambda)^{3\epsilon}\right]^{1/2}, \tag{34}$$

where $\bar{r}_\lambda = r_\lambda/(y_c f_0)$. (Here we can treat f_0 and c_1 as constants evaluated at the limiting $R = \delta_\lambda y_c$). The above profile shows that in a universe dominated by a cosmological constant, the mass of halos is again convergent. We caution that the above forms for the outer profile of halos in open models (viz. Eq. (31) and (34)), obtain only near the cutoff radius and only at late times, as the outermost bound shell turns around only as $t \to \infty$. For a finite fixed time t and general r_i a more detailed solution of (24) and (32) is needed, for finding the density profile. Of course in the innermost regions, the λy^2 term in (32) is expected to be small compared to $1/y$ term, and we will recover the results of the flat model, discussed above and in Section 3. We now turn to the study of halo properties through direct cosmological N-body simulations.

5. Halo properties through cosmological N- body simulations

In order to clarify the effect of non-linear evolution in determining the structure of dark halo cores, it is best to look at power-law spectra, as this has no special scale, rather than a model like the CDM. We have therefore simulated three power law models with index $n = -2, -1, 0$, with $\Omega_0 = 1$. Each simulation is run using a particle-mesh (PM) code, with 768^3 mesh points and 256^3 particles. Although each model has no intrinsic scale, we choose the box size of each simulation to be comoving $10h^{-1}$Mpc. At the end of the simulation, which we identify with redshift zero, the rms density fluctuations on a $8h^{-1}$Mpc sphere, $\sigma_8 = 1/1.3$ in the $n = -2$ model, while in the $n = -1$ model, $\sigma_8 = 1/1.5$ and in the $n = 0$ model, $\sigma_8 = 1/4$. Thus, in all cases waves larger than the box size have typically not grown to the non-linear domain. We will use this scale notation to facilitate discussions at the relevant scales. The nominal spatial resolution of the simulations is $13h^{-1}$kpc, adequate for resolving the galaxy size halos that we are interested in here. The mass of each particle is $1.65 \times 10^7 h^{-1}$M$_\odot$. Thus a galaxy size halo would contain of order 10^5 particles, essential for our purpose of computing density and velocity dispersion profiles. The highest mass resolution in the present simulations is also required to avoid two-body relaxation in the inner regions of halos, which we are most interested in. Within the innermost bin of our calculation ($10h^{-1}$kpc, see below) at an overdensity of about 10^5 (see Figures (2,3,4) below) there are of order thousand particles, thus two-body relaxation should be negligibly small (see also Eq. (36) below).

In each simulation, the center of each halo is selected as the local maximum of the mass distribution within spheres of comoving radius of $10h^{-1}$kpc. The density profile of each halo is calculated using spherical averaging with a logarithmic bin size of 0.02 dex. The velocity dispersions (both tangential and radial) are computed in the restframe of each spherical shell. We have used the density and velocity dispersion profiles of 20 halos in each model for the analysis to be described below. In particular we would like to examine if the halo density profiles show evidence for the scaling laws of Section 2 and 3, and a dependence on the power spectrum.

In our analysis of the halo density profiles, for each halo we first fitted $\rho(r)$, by a double power law model of the form given by

$$\rho(r) = \left(\frac{r_c}{r}\right)^{\alpha_0} \frac{\rho_0 2^{\beta_0}}{[1 + (r/r_c)]^{\beta_0}}. \tag{35}$$

We used the log density versus log radius data, taking all radii within a nominal "virial radius", say r_v, where the density dropped to about 200 times the background density. We made these fits by using an IDL routine (curvefit) which takes a trial model set of parameters and iterates them to minimize the squared sum of the deviations of the fit from the actual density profile. By judicious choice of the starting values of the parameters, it is relatively simple to obtain good convergence in the set of model parameters. The density profile of the 20 halos in each model $n = 0$, $n = -1$, and $n = -2$ are shown as dotted lines in Figures 2, 3 and 4 respectively. (Here the density has been normalised with respect to $\rho_c = \rho_b(t_0)$, the background density at the present epoch t_0). The converged model fit is also shown as a light solid line in these figures. One can see from the figures that, in general, the double power law fit is excellent. Infact, for every halo, the fractional deviations, of the actual $\log(\rho)$ compared to the model fit, are very small; in general much less than 1% for most radii, with maximum deviations less than a few percent. Further as in these fits one minimizes the total least square deviations of the data from the fitted profile, the fitted function is moderately robust to local perturbations in the density. We can therefore use the model fitted profiles to study the properties of halo density profiles.

For each halo, we then calculated the local power law slope of the density profile by evaluating, $s(r) = d(ln\rho)/d(lnr)$, from the model fit. We plot this local slope, $s(r)$, for every halo, as a thick solid line in the same plot as the density profile plot, in Figures 2, 3 and 4. These $s(r)$ plots give the most detailed information regarding the slope of the halo density profiles. If the density profile has a power law regime, then for this radius range, $s(r)$ would be a straight horizontal line. Some general conclusions can be drawn from the figures themselves. First for almost all the halos, $s(r)$ keeps increasing monotonically with radius; showing that the halo density profiles are in general curved, and that the density profile keeps steepening with radius. Previous workers like NFW have in general adopted model double power law profiles to fit halo density profiles, with specific values of the inner slope $\alpha_0 = 1$ and outer slope $\beta_0 + \alpha_0 = 3$. We find the hetrogeneity of the density profiles to be striking. No simple formulae with fixed (α_0, β_0) can fit this data. Indeed for an unbiased double power law fit, the innermost value of $s(r)$ lies between $1 - 2$, shows a general increase with increasing n, and is in general not equal to 1. Also, the outermost value is generally

not equal to 3.

In order to quantify these conclusions better, and since we have a moderately large (20) number of halos in each model, we can infact look at the the statistics of the inner core and outer slopes, for each model of structure formation (given by the power spectrum index n). We do this by looking at the distribution of $s_i(r_0)$ and $s_i(r_v)$ for the 20 halos in each model with a given value of n. Here $s_i(r)$ is the slope function of the i'th halo in a given model, calculated from the model fit, and r_0 is some fiducial characteristic inner radius of a halo.

In Figure 5, we have given a histogram of the distribution of the inner core slopes $s(r_0)$, for the different models of structure formation with $n = 0, -1$ and -2, adopting three different values for r_0. In the left hand side of this plot, we have taken r_0 to be the innermost radius r_i of the halo, in the middle histograms we have taken it to be a fixed percentage (10%, say) of the virial radius, with $r_0 = 0.1 r_v$, while in the right most histograms have taken a larger value $r_0 = 0.15 r_v$. For all the halos in the $n = -1$, or $n = 0$ models, these 3 choices correspond to progressively larger and larger value of r_0. For $n = -2$ case for about half the halos, the innermost radius r_i is of order $0.1 r_v$; hence the close similarity of the histograms for these two cases. The solid arrow in each of these histogram plots shows the location of the median value of the distribution. We also show for comparison by a thin arrow, the location of the core-slope $\alpha_n = 3(3 + n)/(5 + n)$, expected on the basis of the scaling arguments of section 2.

From this figure we see first that all halos do have a cuspy inner density profile, mostly with $s(r_0) > 1$. Further, the core slopes show a clear spectral index dependence although the inner power laws are all somewhat steeper than the $\alpha_n = 3(3 + n)/(5 + n)$ form, predicted by the scaling laws. For example, the median value of the core slope for the $n = -2$ models is $s(r_i) \sim 1.3$ (leftmost histogram), (compared to $\alpha_n = 1$), while for the $n = -1$ and $n = 0$ models, the corresponding median value of the core slope shifts to $s(r_i) \sim 1.6$ ($\alpha_n = 1.5$) and $s(r_i) = 1.8$ ($\alpha_n = 1.8$), respectively. For any fixed n, there is also a systematic increse of the median slope as one increases r_0 and goes from the left-most to the right most histogram. This is to be expected as we have a curved and continuously steepening density profile. However the trends between different models remain (a steeper inner profile for larger n). This can be seen already for example by comparing the left and right side of Figure 5.

Further, we checked using the Kolmogorov-Smirnov two-sample test whether the distribution of core slopes $s(r_i)$ for different values of n, are drawn from the same population or not. We used the one-tailed test to decide if the vaues in one sample (say $n = 0$) are stochastically larger than the values of the other sample (say $n = -2$). In this test one computes the two-sample statistic $D_{M,N} = max[S_M(X) - S_N(X)]$, where $S_M(X), S_N(X)$ are the cumulative probability distributions of the two samples with M and N number of points respectively in each sample (in our case $M = N = 20$). The value of $NMD_{M,N}$ being larger than a given number is then used to rule out the hypothesis (that the samples are drawn from the same population) at various levels of confidence (cf. Siegel and Castellan 1988, pg. 144). This test shows that the distribution of

core slopes of the $n = 0$ model is stochastically larger than the core slopes of the $n = -2$ model, and not drawn from the same population, at a 99% confidence level. The hypothesis that the core slopes of the $n = -1$ and $n = -2$ are drawn from the sampe population is ruled out at a weaker 90% confidence level. And the hypothesis of the core slopes of $n = 0$ and $n - 1$ models being drawn from the same population is ruled out at a $90 - 95\%$ confidence level, depending on the binning used for the data. Our preliminary conclusion, therefore, from analyzing these cosmological N-body simulations (cf. Figures 2 - 5), is that the core density profiles of dark matter halos, do depend on the initial power spectrum of density fluctuations; becoming steeper as the spectral index increases from $n = -2$ to $n = 0$.

In Figure 6, we have given the corresponding histogram for the distribution of the outer slopes $s_i(r_v)$, for different models of structure formation. We see from the figure that the distribution of outer profiles is fairly broad. For the models with $n = 0$ and $n = -1$, they are spread, with large deviations, about a median value $s(r_v) = 3.06$ and $s(r_v) = 3.02$ respectively. For the halos in the $n = -2$ simulation the outer profile is somewhat shallower, being spread around a median value $s(r_v) = 2.55$. These results for the outer profile suggest a large scatter about the favored NFW value of $\beta_0 + \alpha_0 = 3$.

We have summarised the information on the core and outer slopes of dark matter halos, in different models, as a scatter plot in Figure 7. Each point in these scatter plot marks the value of the inner core and outer slope for a particular halo. We also show as a solid cross the location of the median value of the distributions of slopes, with the extent of the cross giving the $\pm\sigma_m$ error on the median. (We adopt an error on the median $\sigma_m = c_N \sigma_N / \sqrt{N}$, where σ_N is the standard deviation of the N values of the the slope distribution and $c_N = 1.214$ (cf. Kendall and Stewart 1963, pg 327). This figure further illustrates the result that the distribution of the core and outer slopes have a large scatter but appear to display systematic trends as one goes from $n = 0$ to $n = -2$.

At this point we should add a note of caution regarding the determination of the inner slopes. Ideally for determining the inner core properties one has to have a resolution as small as possible and as many particles within the virial radius as possible, though it is not at present clear what these numbers should be. In the biggest halos we have few times 10^5 particles; and our resolution in these halos is about $5 - 7.5\%$ of the virial radius. The larger resolution scale is because we have extracted halos from a cosmological PM simulation, though it is one of the best resolved PM simulation (with a 768^3 mesh). Of course one advantage of the present work is that we have a large number of halos (20) in each model, and so can look at the halo properties in a statistical fashion as well. And we saw above that the statistical analysis reveals the trend in core slopes, more clearly. At the spatial resolution of the current simulations, the overdensity is about $10^4 - 10^5$, which is about the overdensity of real galaxy or cluster halos on the same scale. Therefore, our simulations may not be severely spatial resolution limited for the present purpose of examining the properties of halos on these scales and larger. Still, it would be very useful to see whether the trends we have found here for the core slope, hold up with further high resolution

studies of a large number of halo density profiles. In particular, it will be of great interest to go to even higher overdensity, more inner regions of halos using higher mass and spatial resolution simulations to further test the present findings from simulations as well as our analytic results.

Apart from the density profiles, it is also of interest to study the velocity dispersion profiles of the halos, to see if there is any evidence for undigested cores. As we argued in section 2 and 3, this will lead to a rising velocity dispersions in the core regions, of the form $\sigma \propto r^{(1-n)/(2(5+n))}$, which also implies a mild but systematic spectral dependence. It is also of interest to check the relative importance of tangential and radial dispersions in the halo. Recall from the work of section 3, that tangential dispersions are needed to get cuspy density profiles shallower than $1/r^2$ in self similar collapse from power law initial density profiles; and that a cuspy profile shallower than $1/r$ required tangential dispersions to dominate radial dispersion. Our data on the velocity dispersion profiles are too noisy for drawing very firm conclusions. However we do find most halos showing a rise in the radial velocity dispersion with increasing radius in the core regions. Further, the tangential dispersions are smaller than radial and also in general show much weaker (sometimes no) rise with increasing radius in the core.

One may wonder about the importance of 2-body relaxation effects in determining the properties of the halo cores in the simulation; for example significant 2-body relaxation could lead to an artificial steepening of the density profiles of the halos in the core regions. We can use the halo properties in the simulation itself to check this, using the standard estimate for the 2-body relaxation time scale t_{rel} (cf. Binney and Tremaine, 1987 (Eq. 8.71); see also Steinmetz and White 1997), and comparing it with the Hubble time $t_{hub} = t_0$. We obtain

$$\frac{t_{rel}}{t_{hub}} = 11.8 h^{-1} \left(\frac{\sigma}{\sigma_*}\right)^3 \left(\frac{m_*}{m}\right) \left(\frac{(\rho/\rho_b)}{d_*}\right)^{-1} \left(\frac{\ln(\Lambda)}{10}\right)^{-1}, \tag{36}$$

where we have taken fiducial values $\sigma_* = 200$ km s^{-1}, $m_* = 1.65 \times 10^7 M_\odot$, $d_* = 4 \times 10^4$, and $\ln(\Lambda)$ is the usual "coulomb" logarithm, which is of order 10. In general we find this number is much larger than unity for all halos, even in the innermost regions. So 2-body relaxation is not expected to be important in the halo cores.

6. Discussion and Conclusions

We have concentrated in this work on the structure of the cores of dark halos in hierarchical clustering theories of galaxy formation. In such theories, it is very likely that cores of dark matter halos harbor undigested earlier generation material. Their density structure, in physical as well as phase space, will reflect the times and the cosmological densities when the core material was gathered.

In a flat universe with a power spectrum $P(k) \propto k^n$, a consequence of undigested cores, could be a cuspy core density profile, shallower than that of a singular isothermal profile, having

a velocity dispersion profile and rotation curve, which rises with increasing radius. Scaling arguments, incorporating energy and mass conservation, suggests a form for the core density profile, $\rho(r) \propto r^{-\alpha_n}$, with $\alpha_n = (9 + 3n)/(5 + n)$. This profile will transit to a steeper power law, determined by say secondary infall, beyond the core radius. The core radius, which is also the radius, where the density has an effective logarithmic slope of -2, is related to and a fraction of the turn around radius for the matter infalling to the halo. The characteristic density at this radius is a few hundred times the turn around density, and therefore correlates inversely with typical halo mass, and directly with the halo formation redshift.

Although scaling laws suggest a possible form of the core density profile, they do not tell us how and in fact whether this form will be realized dynamically. To explore this dynamical issue, we have adopted two complimentary approaches. First, in section 3, we studied a simple tractable model: The spherical self similar collapse of dark matter density perturbations, in a flat universe. Then in section 5, we analyzed the properties of halos obtained in some cosmological N-body simulations, with a power law spectrum of density fluctuations.

The problem of spherical self similar collapse, has often been solved earlier by following particle trajectories. We adopted instead another approach, examining directly the evolution of the moments of the phase space density. For a purely radial collapse, with the initial density profile $\propto r^{-3\epsilon}$, and steeper than r^{-2}, we recover, by demanding that the core be static, the asymptotic form of the non-linear density profile: $\rho \propto r^{-\alpha} \propto r^{-9\epsilon/(1+3\epsilon)}$ (see also Padmanabhan 1996b). For initial density profiles shallower than $1/r^2$, with $\epsilon < 2/3$, we showed that, non radial velocities are necessarily required to obtain a static core. These results agree with the work of B85 and FG who followed particle trajectories to solve this problem.

The consequences of introducing non radial velocity dispersions, in this approach, can only be examined, by adopting a closure approximation to the moment equations. In the spherical collapse problem, the skewness of the tangential velocities can be assumed to be zero, in the core regions. Infact, in regions where large amounts of shell crossing has occurred, one can assume that a quasi "equilibrium" state obtains, whereby all odd moments of the distribution function, over $(\mathbf{v} - \bar{\mathbf{v}})$, may be neglected. One can then analytically integrate the Jeans equation for the self similar collapse, including the effect of tangential velocity dispersions. For an initial density profile shallower that $1/r^2$, with $\epsilon < 2/3$, a static core with a non-linear density profile, with $\alpha = 9\epsilon/(1 + 3\epsilon)$, is possible, only if the core has sufficiently large tangential velocity dispersions. In fact, one needs $\bar{v_\theta^2} > GM/2r$. Also if a static core has to have a cuspy density profile shallower than $1/r$, (with $\alpha < 1$), one requires $\bar{v_\theta^2} > \bar{v_r^2}$. Importantly for the case $3\epsilon = (3 + n)/2$ (as would be relevant for collapse around a typical point in the universe), we recover the simple result $\alpha = \alpha_n = (9 + 3n)/(5 + n)$, with $\alpha_n < 2$, for $n < 1$.

Note that the radial peculiar velocity which could have negligible skewness in the core, will necessarily have a non-zero skewness (non zero third moment) near a caustic radius, where collapsing dark matter particles meet the outermost shell of re-expanding matter. In a companion

paper (S99), to take this into account, we have introduced the following fluid approach. In this approach, the effect of peculiar velocity skewness are neglected in all regions except at location of the caustic, which we call the shock. In the particle picture the shock is where a single stream flow becomes a muti stream flow. In the fluid picture it is a where some of the average infall velocity (of the single stream flow), is converted to velocity dispersion (of the multi stream flow). The location of the caustic, y_s, in scaled co ordinates, is found as an eigenvalue to the problem of matching the single stream collapse solution at $y > y_s$, with a static core solution within $y << y_s$, as determined here. This is done in S99 by numerically integrating the full set of moment equations. The results largely bear out the expectations of section 3; the importance of tangential velocity dispersions, in deciding the nature of the core density profile. For the details please see S99.

The above results and that of S99, although derived for the case of a purely self similar collapse, illustrate the importance of dynamical considerations, in determining the structure of halo cores. They illustrate features which are like to obtain in more realistic collapse: If newly collapsing material is constrained to mostly contribute to the density at larger and larger radii, then memory of initial conditions can be retained. In the more general case, when newly collapsing material is able to occupy similar regions as the matter which collapsed earlier, the core density profile will only partially reflect a memory of the initial conditions.

The density profiles of the outer regions of dark halos are briefly studied in Section 4, relaxing the restriction to a flat universe and following the Gunn-Gott paradigm. For an open universe and at late times, the outer density profile goes over to a limiting form $\rho(r) \propto r^{-4}$, where the slope is independent of the power law slope of the initial density profile. The corresponding limiting outer profile for a Λ dominated universe was shown to have a form $\rho(r) \propto [1 - (r/\bar{r}_\lambda)^{-3\epsilon}]^{1/2}$, where $\bar{r}_\lambda$ is a characteristic cut-off radius. These density profile laws show that in open and Λ dominated models, the halo mass is convergent and halos have characteristic density cut-off's, which may be observationally testable.

We then turned to a complimentary approach, of looking at halo properties in numerical simulations of structure formation models with a power spectrum $P(k) \propto k^n$; with 3 different values of the spectral index $n = -2, -1, 0$, and with $\Omega_0 = 1$. The results are summarized in figures 2 - 7. One preliminary conclusion, is that the core density profiles of dark matter halos, do depend on the initial power spectrum of density fluctuations; with the local core slope becoming steeper as the spectral index increases from $n = -2$ to $n = 0$.

For example, the median value of the inner core slope $s(r_i)$ for the $n = -2$ models is 1.3 ± 0.07, while for the $n = -1$ and $n = 0$ models, the corresponding median value of the core slope shifts to 1.6 ± 0.09, and 1.8 ± 0.09 respectively. For any fixed n, there is also a systematic increse of the median slope as one increases r_0 and goes from the left-most to the right most histogram in Figure 5. These values are generally steeper than $\alpha_n = 1, 1.5$ and 1.8, which scaling arguments predict for models with $n = -2, -1$ and 0 respectively. Further the Kolmogorov-Smirnov two sample test shows that the distribution of core slopes of the $n = 0$ model is stochastically larger than the core

slopes of the $n = -2$ model, and not drawn from the same population, at a 99% confidence level. It also rules out the hypothesis that the core slopes of the $n = -1$ and $n = -2$ models (or the $n = 0$ and $n = -1$ models) are drawn from the sampe population, at a weaker 90% confidence level. The NFW value of $\alpha_0 = 1$ is not favored; most halos having a steeper core density profile. Some recent higher resolution simulations, of cluster and galactic scale dark halo formation in the CDM model, by Moore *et al.* (1998, 1999), which resolve the core very well (but only for a few halos), has also obtained a core profile $\rho \propto r^{-1.5}$, steeper than the NFW profile.

The velocity dispersion profiles of halo cores, in the N-body simulations are somewhat noisy, but do indicate for most halos a rise in the radial velocity dispersion in the core regions. The tangential dispersions are smaller than radial and also in general show much weaker (sometime no) rise in the core. The Moore *et al.* (1998) cluster halo also shows a rise in the velocity dispersions in the core (Moore, private communication). Indeed Moore *et al.* (1998) point out that a significant fraction of the core material is made from high density material which collapsed at higher redshift. It would be very useful to see in the future whether these trends hold up with large statistical studies of halo density profiles, with higher spatial resolution.

An understanding of what determines the core density profiles of dark halos is important for several issues. Perhaps one of the most relevant and dramatic effect will be on strong gravitational lensing properties of galactic and clusters scale dark matter halos. For example the multiple imaging lensing cross sections will be very different whether one has $\alpha = 0, -1$ or $\alpha = -2$. Compare the work of Subramanian, Rees and Chitre (1987) where the lensing cross section by dark halos was estimated assuming that they have soft cores with the work of Narayan and White (1988) where halos were assumed to be singular isothermal spheres.

More specifically, a given system is capable of producing multiple images if its surface density exceeds a critical value Σ_c (Turner, Ostriker and Gott 1984; Subramanian and Cowling 1986). For $\alpha \geq 1$ the surface density is divergent in the central regions. So, generically, if $\alpha \geq 1$, *all* clusters are capable of producing multiple images. For $\alpha < 1$, some clusters can produce multiple images and some can not. The NFW value of $\alpha = 1$ is at the boundary with surface density logarithmically singular. Thus the actual values of α for real systems is quite relevant to the frequency of strong lensing. As the frequency of multiple images from gravitational lensing also provides a powerful independent test of cosmological models, (cf. Cen *et al.*, 1994, Wambsganss, Cen and Ostriker 1998, Cen 1998), it is important to determine the structure of halo cores. Further, the existence and properties of radial arcs, which have been observed in some cluster scale lenses depends on the slope of the inner cusp (cf. Mellier, Fort and Kneib 1993, Miralda-Escude 1995, Bartelmann 1997, Evans and Wilkinson 1998). For the singular isothermal profile and stronger cusps, radial arcs do not form.

The rotation curves of disk galaxies also holds clues to the core density profile of dark halos. But it is more difficult to decompose the observed rotation curve unambiguously into contributions from the luminous stellar disk/bulge and the dark halo. The fluid approach adopted

in section 3 and in S99 raises a new way of exploring non linear dynamics, which can extend analytic approximations like the Zeldovich approximation, valid in a single stream flow, to the multi streaming regime. In the fluid approach multistreaming regions would correspond to regions with velocity dispersions, generated by the Zeldovich type caustics. Note that the adhesion approximation, is one extreme where the multi streaming regions are collapsed onto a caustic. It would be interesting to explore this issue further. In this work we have not included the dynamics of the gaseous (the baryonic) component, which will be in fact relevant for the interpretation of x-ray observations of clusters. The gas necessarily has an isotropic velocity dispersion, and so will have a different dynamical evolution compared to the dark matter. We hope to return to some of these issues in the future.

REFERENCES

Bardeen, J. M., Bond, J. R., Kaiser, N., and Szalay, A. S., ApJ, 304, 15.

Barrow, J. D., and Saich, P. 1993, MNRAS, 262, 717.

Bartelmann, M., 1996, Astron. Astrophys., 313, 697.

Bertschinger, E. 1985, ApJS, 58, 39.

Binney, J., and Tremaine, S., 1987, Galactic Dynamics, Princeton University Press.

Cen, R., Gott, J. R., Ostriker, J. P. and Turner, E. L., 1994, ApJ, 423, 1.

Cen, R., 1998, ApJ, 509, 16.

Cole, S. M., and Lacey, C., 1996, MNRAS, 281, 716.

Chieze, J-P, Teyssier, R., and Alimi, J-M, 1997, ApJ, 484, 40.

Evans, N. W. and Wilkinson, M. I., 1998, MNRAS, 296, 800.

Fillmore, J. A., and Goldreich, P. 1984, ApJ, 281, 1.

Fukushige, T., and Makino, J. 1997 ApJ, 477, L9.

Gunn, J. E., 1977, ApJ, 218, 592.

Gunn, J. E., And Gott, J. R., 1972, ApJ, 176, 1.

Henriksen, R. N., and Widrow, L. M., 1997, Phys. Rev. Lett., 78, 3426.

Hoffman, Y., and Shaham, J. 1985, ApJ, 297, 16.

Huss, A., Jain, B., and Steinmetz, M. 1997, preprint (astro-ph/9703014)

Huss, A., Jain, B., and Steinmetz, M. 1999, ApJ, 517, 64.

Kendall, M. G., and Stuart, A. 1963, The advanced theory of statistics, Charles Griffin and Company Limited, London.

Kravtsov, A. V., Klypin, A. A., Bullock, J. S., and Primack, J. R., 1998, ApJ, 502, 48.

Kumar, A., Padmanabhan, T., and Subramanian, K. 1995, MNRAS, 272, 544.

Lahav, O., Lilje, P. B., Primack, J. R., and Rees, M. J. 1991, MNRAS, 251, 128.

Mellier, Y., Fort, B. and Kneib, J.-P., 1993, ApJ, 407, 33.

Miralda-Escude, J., 1995, ApJ, 438, 514.

Moore, B., Governato, F., Quinn, T., Stadel, J., and Lake, G. 1998, ApJL, 499, L5.

Moore, B., Quinn, T., Governato, F., Stadel, J., and Lake, G. 1999, preprint (astro-ph/9903164).

Narayan, R. and White, S. D. M., 1988, MNRAS, 231, 97.

Navarro, J. F., Frenk, C. S., and White, S. D. M. 1995, MNRAS, 275, 720.

Navarro, J. F., Frenk, C. S., and White, S. D. M. 1996, ApJ, 462, 563.

Navarro, J. F., Frenk, C. S., and White, S. D. M. 1997, ApJ, 490, 493.

Nusser, A, and Sheth, R. K., 1999, MNRAS, 303, 685.

Padmanabhan, T. 1993, Structure formation in the universe, Cambridge University Press.

Padmanabhan, T. 1996a, Cosmology and astrophysics through problems, Cambridge University press.

Padmanabhan, T. 1996b, MNRAS, 278, L29.

Padmanabhan, T. and Subramanian, K. 1992, Bull. Astr. Soc. Ind., 20, 1.

Peebles, P. J. E., 1980, The Large Scale Structure of the Universe, Princeton University Press.

Sikvie, P., Tkachev, I. I., and Wang, Y. 1997, Phys. Rev. D, 56, 1863.

Siegel, S., and Castellan, 1988, Non parametric statistics for behavioural sciences, McGraw-Hill.

Steinmetz, M., and White, S. D. M. 1997, MNRAS, 288, 545.

Subramanian, K., 1999, ApJ(submitted) (S99).

Subramanian, K., and Cowling, S. A. 1986, MNRAS, 219, 333.

Subramanian, K., Rees, M. J. and Chitre, S. M., 1987, MNRAS, 224, 283.

Syer, D., and White, S. D. M., 1998, MNRAS, 293, 337.

Thomas, P. A., *et al.*, 1998, MNRAS, 296, 1061.

Tormen, G., Bouchet, F. R., and White, S. D. M. 1997, MNRAS, 286, 865.

Wambsganss, J., Cen, R. and Ostriker, J. P., 1998, ApJ, 424, 29.

White, S. D. M., and Zaritsky. 1992, ApJ, 394, 1.

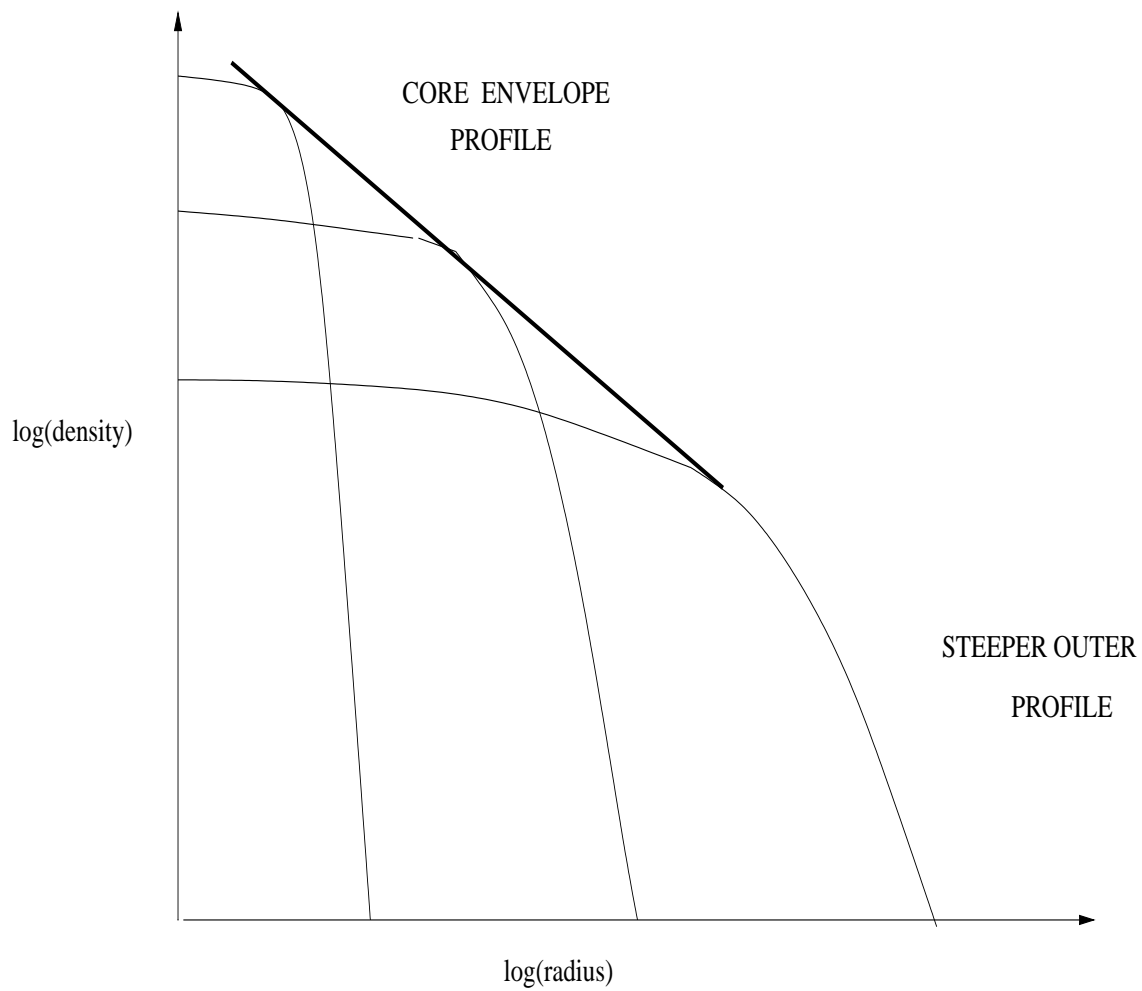Xu, G. 1995, Phd Thesis, Princeton University.

Fig. 1.— Schematic illustration of how the density profile of a large halo core could arise as an envelope of the density profiles of undigested cores of smaller mass halos.
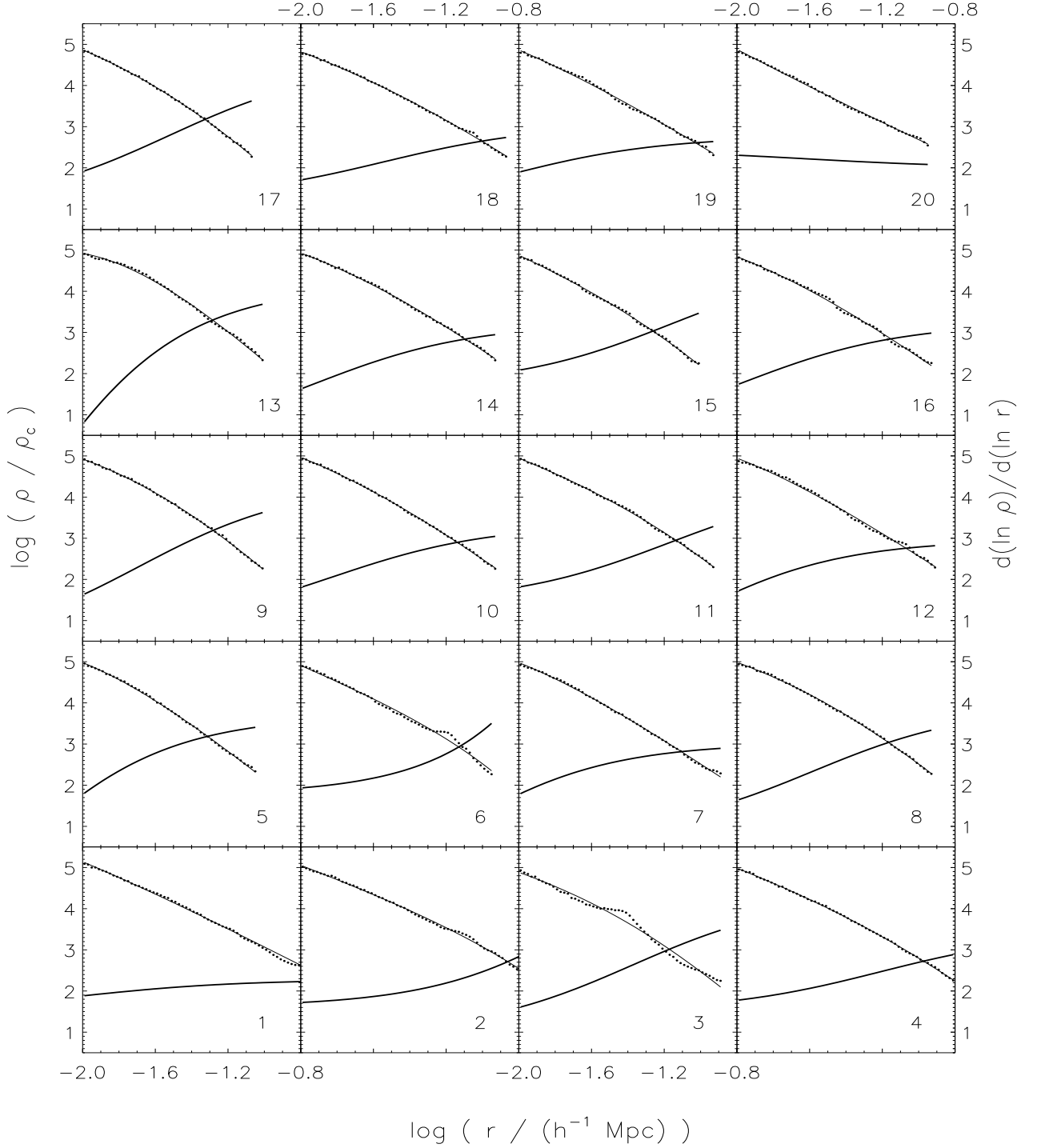
Fig. 2.— The density profiles of the 20 halos in N-body simulations with $n = 0$, are shown as dotted lines in each panel. The halos are numbered in each panel for easy identification. A double power law fit to each density profile data is superposed as a light solid line in these figures. For each halo, the local logarithmic slope of the density profile, $s(r) = d(ln\rho)/d(lnr)$, calculated from the model fit is shown as a thick solid line, in the same plot as the density profile plot.
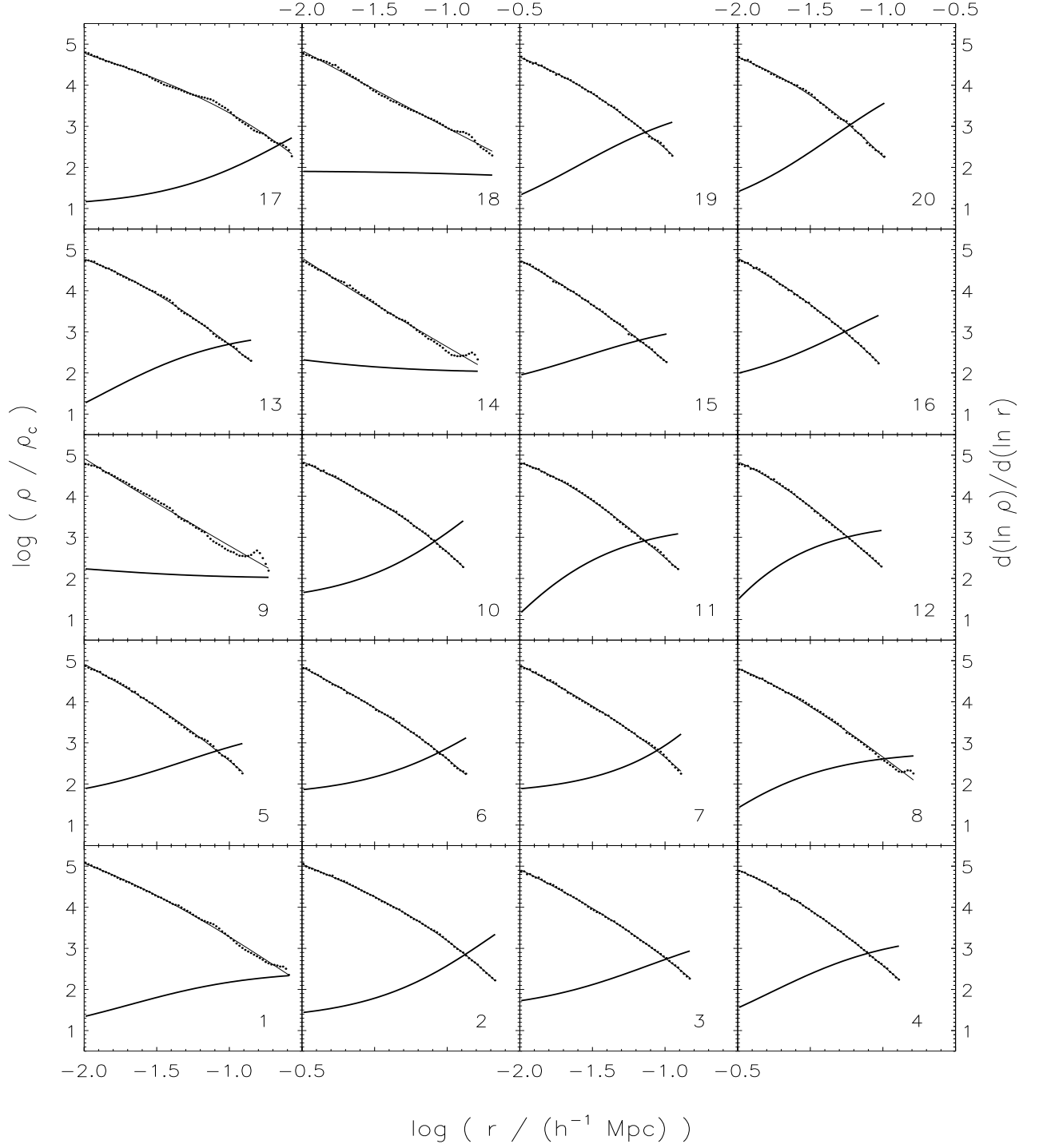
Fig. 3.— The density profiles and the logarithmic slopes for the 20 halos in the simulation with $n = -1$. The dotted line, thin solid line and thick solid line as as in Fig. 2.
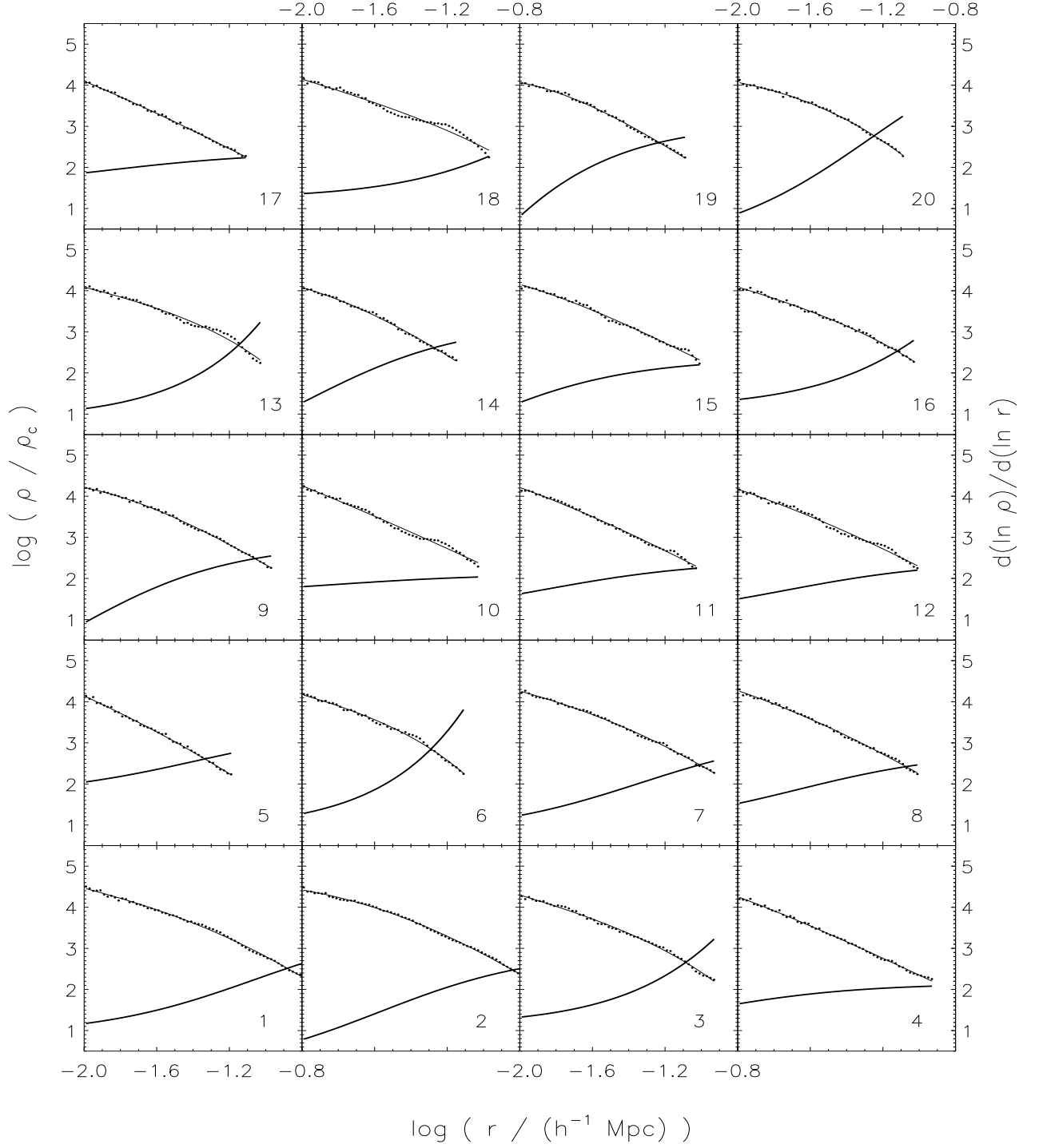
Fig. 4.— The density profiles and the logarithmic slopes for the 20 halos in the simulation with $n = -2$. The dotted line, thin solid line and thick solid line as as in Fig. 2.
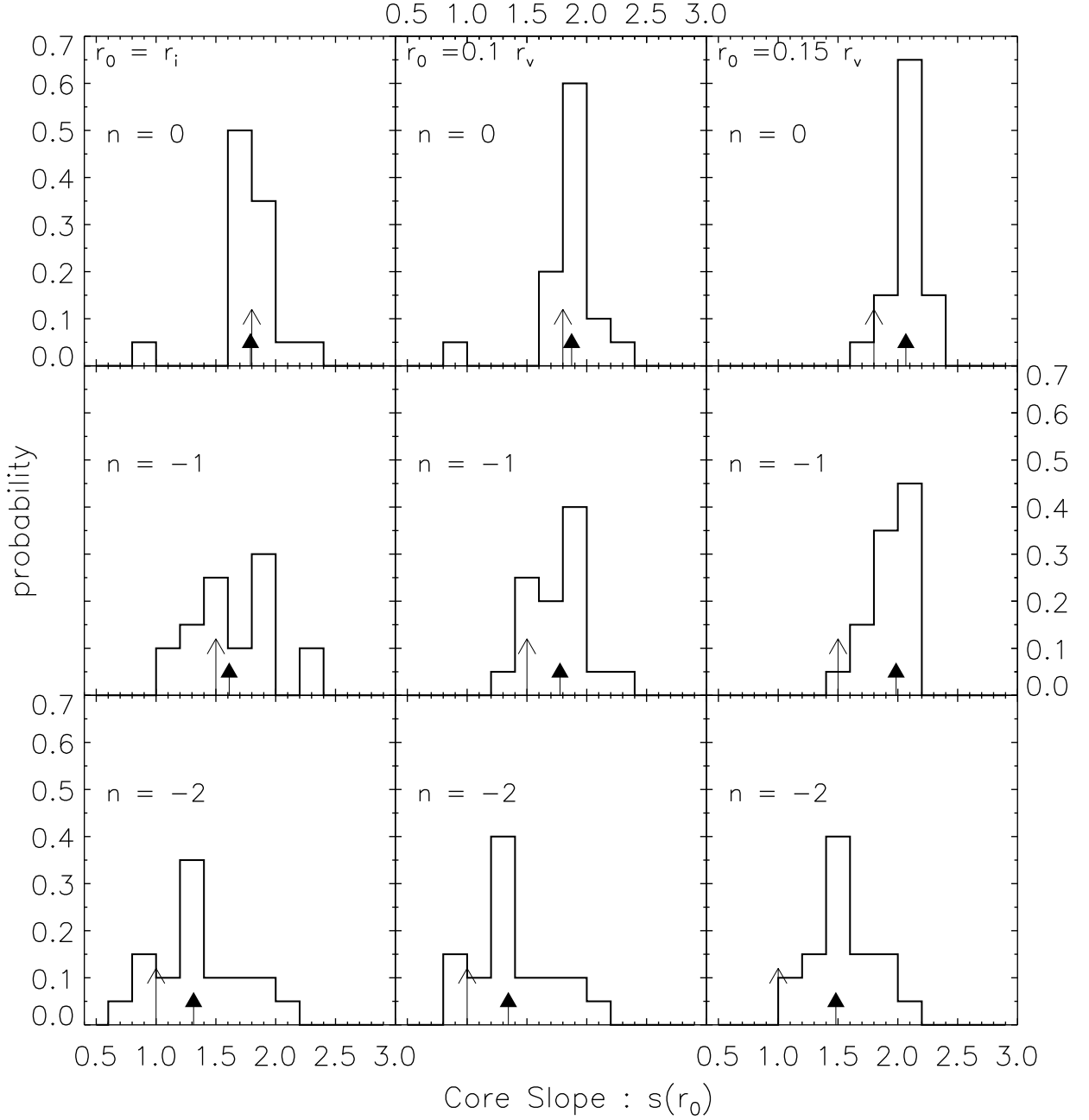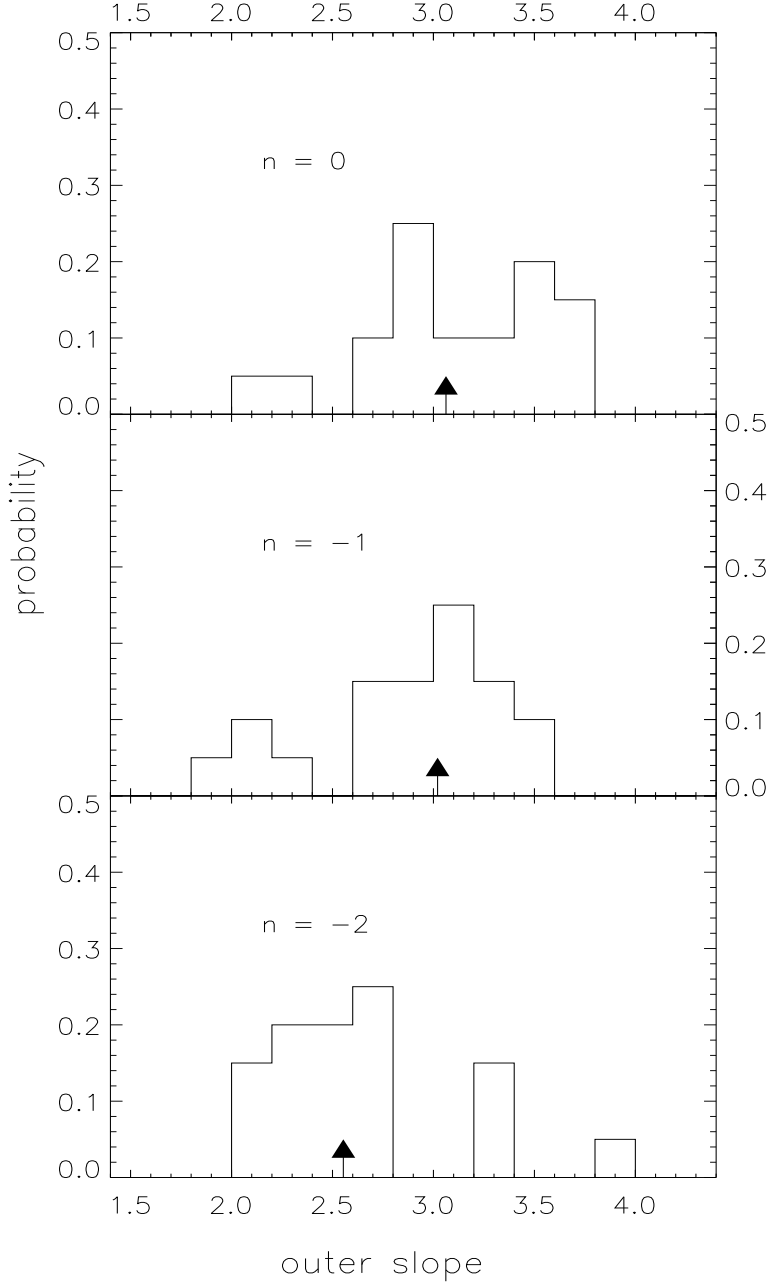
Fig. 5.— The distribution of core slopes of halo density profiles in different models. The solid arrow shows the location of the median of the distribution while the thin arrow indicates the location of the value $3(3 + n)/(5 + n)$, predicted by scaling arguments.

Fig. 6.— The distribution of outer slopes of halo density profiles in different models. The solid arrow shows the location of the median of the distribution.
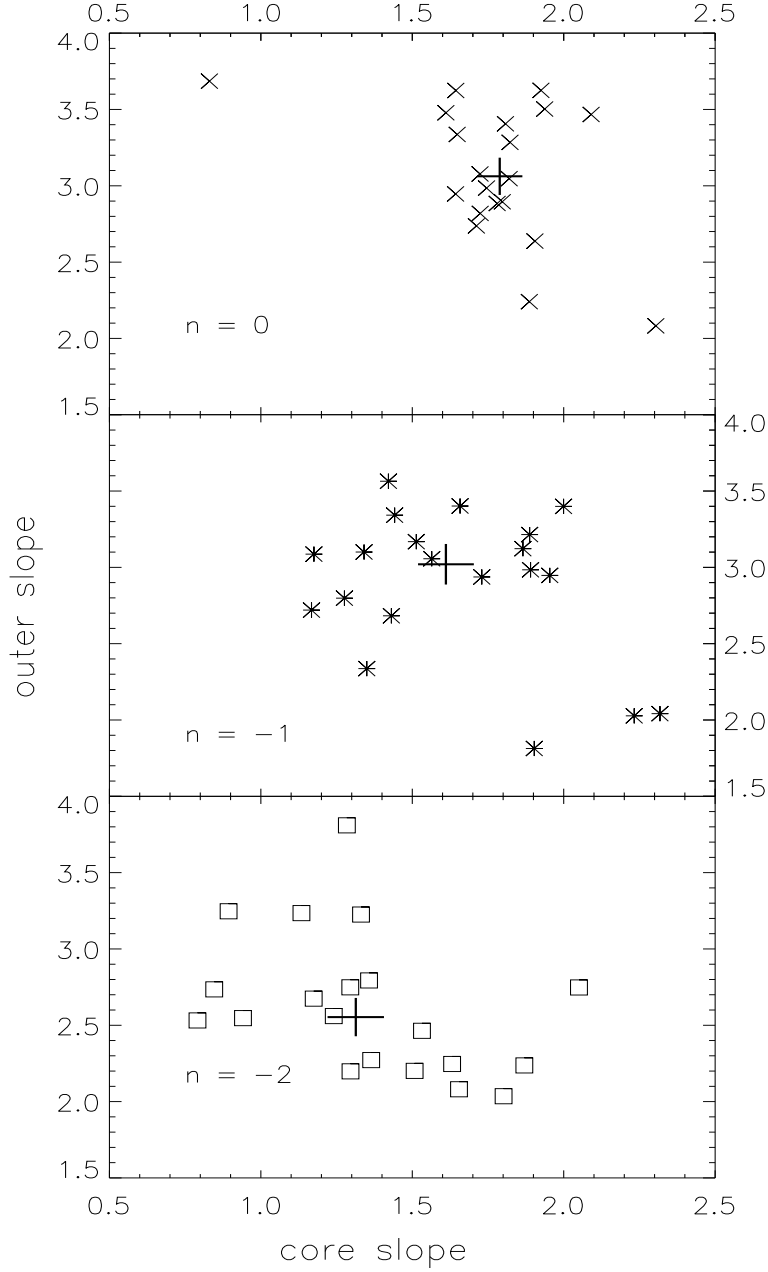
Fig. 7.— The distribution of the inner core and outer slopes of halo density profiles in different models. The cross marks the median value of these slopes and its extent gives the ± error on the median values.